J. Phys. B: At. Mol. Opt. Phys. 24 (1991) L653–L659. Printed in the UK

LETTER TO THE EDITOR

Spin-resolved superelastic scattering from sodium at 10 and 40 eV

R E Scholten, S R Lorentz, J J McClelland, M H Kelley and R J Celotta

Electron and Optical Physics Division, National Institute of Standards and Technology, Gaithersburg, MD 20899, USA

Received 17 October 1991

Abstract. Spin-resolved superelastic electron scattering from sodium has been measured at total energies of 10 and 40 eV, for scattering angles between 10° and 140°. The angular momentum transfer, $L_\perp$, and the spin-resolved components $L_\perp^T$ and $L_\perp^S$ have been determined. The ratio, r, of triplet to singlet differential cross sections has also been found. The data are compared to theoretical calculations based on close-coupling and distorted-wave models. The spin-averaged $L_\perp$ and triplet $L_\perp^T$ show good agreement with close-coupling theory while the singlet $L_\perp^S$ and the ratio r are poorly predicted.

Sodium has become an important test case for electron–atom collision studies at low energies, both by virtue of its experimental convenience and the simplification it affords to theoretical models. The very strong coupling between the ground and first excited states of sodium suggests the likely success of a close-coupling approximation with only a small number of states (Moores and Norcross 1972). Simpler models have also been used, from Born and Glauber approximations to distorted wave models, including those of Kennedy *et al* (1977), Purohit and Mathur (1990) and Balashov *et al* (1989).

Generally, theoretical calculations predict complex scattering amplitudes for separate spin and angular momentum substate channels. The ultimate goal of experimental tests of such models is a complete determination of the magnitude and phase of these complex amplitudes. Most experiments, however, measure parameters which depend on averages over some or all amplitudes.

Total and differential cross sections provide the least detailed test of theory because they are determined from averages over the largest number of separate channel amplitudes. Examples of such measurements on sodium can be found in the work of Enemark and Gallagher (1972), Shuttleworth *et al* (1977), Srivastava and Vušković (1980), Teubner *et al* (1986) and Lorentz and Miller (1991).

Alignment and orientation parameters provide the next level of detail, and therefore a more critical test of theory. For example, in the natural reference frame of Hermann and Hertel (1982), orientation depends on the relative magnitude of separate angular momentum channel amplitudes, while alignment depends on the relative phase between them. Measurements of these parameters can be made using coincidence techniques, as in Teubner *et al* (1986), or using the equivalent time-reversed superelastic scattering from laser-excited atoms, for example in the early work of Hertel and Stoll (1974). Andersen *et al* (1988) and Slevin and Chwirot (1990) provide extensive reviews of this field.

Alignment and orientation studies can be extended by using spin-polarized collision partners, thereby allowing complete determination of all scattering amplitudes (Hertel *et al* 1987). At low incident energies, exchange effects are expected to play a significant role, and these can be directly probed by resolving spin (Kessler 1985). In some cases, spin-resolved experiments are also sensitive to spin-orbit effects, but in the present case these can be neglected due to the small target atomic number.

We report here measurements of the spin-averaged orientation, $L_\perp$, separate triplet and singlet channel orientations, $L_\perp^{\mathrm{T}}$ and $L_\perp^{\mathrm{S}}$, and the triplet-to-singlet scattering ratio, r. Superelastic techniques have been employed, with spin-polarized electrons and spin-polarized target atoms. Results are presented for total energies of 10 and 40 eV, corresponding to incident electron energies of 7.9 and 37.9 eV, for scattering angles of 10° to 140°. The energies were chosen to maximize the information available for theoretical comparison with respect to previous measurements; 40 eV because it provides spin-resolved data at an energy which is substantially higher than previously reported measurements, while 10 eV was selected to represent a low energy, but above the ionization threshold at 5.14 eV. These data are an extension of the earlier work of McClelland *et al* (1989).

The results have been obtained using an apparatus comprehensively described in a previous publication (McClelland *et al* 1989) and shown schematically in figure 1. Electrons were produced by photoemission from a negative electron affinity GaAs crystal, using circularly polarized light from a diode laser. The electron polarization, perpendicular to the scattering plane, was flipped between up and down states by changing the helicity of the diode laser radiation with a Pockels cell. Mott scattering at 100 keV from a gold foil target (Hodge *et al* 1979) was used to determine the electron polarization P_e of 0.32 ± 0.02.

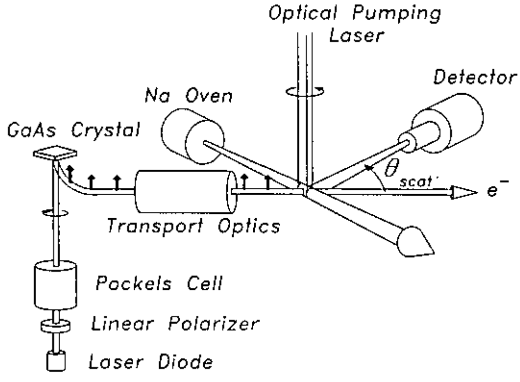

Figure 1. Experimental configuration, showing sodium oven, laser, GaAs polarized electron source, superelastic electron detector and electron scattering angle θ_{scat}.

The electrons were directed at sodium atoms produced by a collimated effusive recirculating oven. The sodium beam was optically pumped with circularly polarized light from a single-mode frequency-stabilized ring dye laser incident perpendicular to the scattering plane. The laser intersected the atom beam in the electron–sodium interaction region to maintain the maximum population of excited-state target atoms.

The atoms were pumped to the $3^2\mathrm{P}_{3/2}F=3$ state and either $M_F=\pm 3$ substate for $\sigma^\pm$ circularly polarized light. Two pumping schemes were used. The $3^2\mathrm{S}_{1/2}(F=2)\rightarrow 3^2\mathrm{P}_{3/2}(F=3)$ transition at $\lambda_0=589$ nm was pumped in both cases, but for the 40 eV results an acousto-optic modulator was used to produce a second collinear beam to pump the $3^2S_{1/2}(F=1)\rightarrow 3^2P_{3/2}(F=2)$ transition at ν_0+1712 MHz ($\nu_0=c/\lambda_0$). Thus atoms normally trapped in the $F=1$ ground hyperfine level were pumped, increasing the excited fraction from approximately 30% to nearly 50% (Lorentz *et al* 1991).

The superelastically scattered electrons, that is those that had gained 2.1 eV in energy through collision with laser-excited atoms, were selected with a retarding field analyser and detected with a channel electron multiplier. The analyser and detector were mounted on a turntable centred on the interaction volume and rotating in the scattering plane.

At each energy and scattering angle, four electron scattering rates were measured, corresponding to the different relative orientations of electrons and atoms. We denote these as $I_{ea}=I_{\uparrow\uparrow}$, $I_{\uparrow\downarrow}$, $I_{\downarrow\uparrow}$ and $I_{\downarrow\downarrow}$ where e and a refer to the direction of electron spin and atom orientation respectively, in a 'natural' reference frame with quantization axis perpendicular to the scattering plane (Hermann and Hertel 1982).

The collision is normally considered in an LM_L basis, since the collision time is much shorter than fine and hyperfine precession times (Percival and Seaton 1958). The optically pumped $F=3$, $M_F=\pm 3$ atomic states can therefore be considered as pure $M_L=\pm 1$ states. In addition, they correspond to states with electron spin up or down, with $M_S=\pm\frac{1}{2}$.

The intensities for *up* and *down* atoms correspond to the populations of the separate $M_L=+1$ and -1 magnetic substates of an ($L=1$) P state, after an equivalent inelastic collision, in the natural frame (Andersen *et al* 1988). Thus, $L_\perp$, the angular momentum transferred to the atom, is found from the relative difference between these intensities, and the unpolarized quantity is obtained by averaging over the incident electron spin:

$$L_\perp=\frac{(I_{\uparrow\uparrow}+I_{\downarrow\uparrow})-(I_{\uparrow\downarrow}+I_{\downarrow\downarrow})}{(I_{\uparrow\uparrow}+I_{\downarrow\uparrow})+(I_{\uparrow\downarrow}+I_{\downarrow\downarrow})}. \tag{1}$$

The spin-dependent quantities are defined in terms of triplet (T) and singlet (S) 'pseudo-intensities' which correct for the incomplete electron spin polarization (Hertel *et al* 1987):

$$T_{11}=(1+P_e)I_{\uparrow\uparrow}-(1-P_e)I_{\downarrow\uparrow} \tag{2}$$

$$T_{-1-1}=(1+P_e)I_{\downarrow\downarrow}-(1-P_e)I_{\uparrow\downarrow} \tag{3}$$

$$S_{11}=(3+P_e)I_{\downarrow\uparrow}-(3-P_e)I_{\uparrow\uparrow} \tag{4}$$

$$S_{-1-1}=(3+P_e)I_{\uparrow\downarrow}-(3-P_e)I_{\downarrow\downarrow}. \tag{5}$$

The spin-resolved angular momentum transfers can then be written as

$$L_\perp^T=\frac{T_{11}-T_{-1-1}}{T_{11}+T_{-1-1}} \tag{6}$$

$$L_\perp^S=\frac{S_{11}-S_{-1-1}}{S_{11}+S_{-1-1}}. \tag{7}$$

The ratio of triplet to singlet scattering differential cross sections, r, is just

$$r=\frac{T_{11}+T_{-1-1}}{S_{11}+S_{-1-1}} \tag{8}$$

which has the value $r=1$ in the absence of exchange.

The results are shown in figures 2 and 3 for 10 and 40 eV respectively. Note that the actual incident electron energies were 7.9 and 37.9 eV. The data are shown with

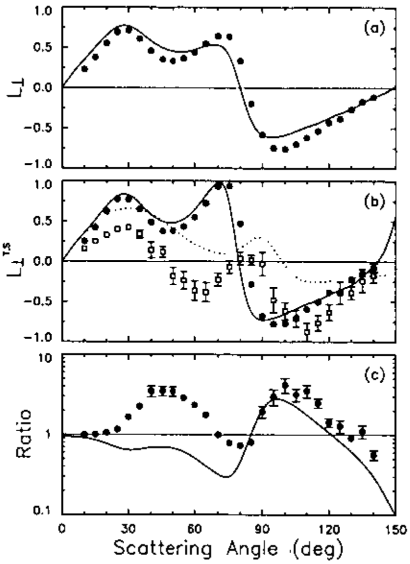

Figure 2. Superelastic electron–sodium scattering with 10 eV total energy. (*a*) Spin-averaged angular momentum transfer, $L_\perp$: ●, present results; ——, 4CC (Mitroy *et al* 1987). (*b*) Spin-resolved angular momentum transfer, $L_\perp^T$ and $L_\perp^S$: ●, $L_\perp^T$ present results; □, $L_\perp^S$ present results; ——, $L_\perp^T$ 4CC (Mitroy *et al* 1987); · · · ·, $L_\perp^S$ 4CC (Mitroy *et al* 1987). (*c*) Triplet-to-singlet ratio, *r*: ●, present results; ——, 4CC (Mitroy *et al* 1987).

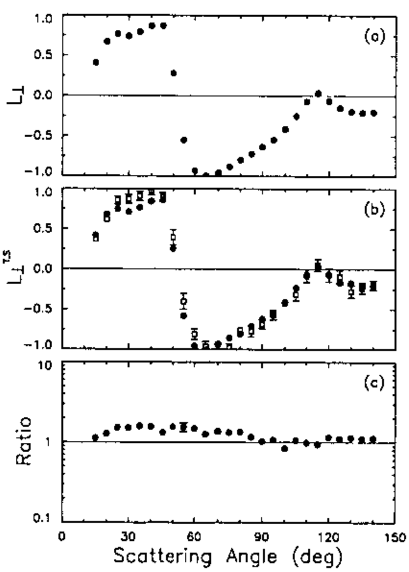

Figure 3. Superelastic electron–sodium scattering with 40 eV total energy. (*a*) Spin-averaged angular momentum transfer, $L_\perp$: ●, present results. (*b*) Spin-resolved angular momentum transfer, $L_\perp^T$ and $L_\perp^S$: ●, $L_\perp^T$ present results; □, $L_\perp^S$ present results. (*c*) Triplet-to-singlet ratio, *r*: ●, present results.

one standard deviation error bars, calculated by propagation of the uncertainty due to counting statistics in the usual manner, as described in the appendix of McClelland *et al* (1989). The error bars are not shown where they are less than the size of the symbols used to represent the data points.

At small angles, both the 10 and 40 eV spin-averaged $L_\perp$ results (figures 2(*a*) and 3(*a*)) show behaviour which can be qualitatively explained by simple classical arguments (Kohmoto and Fano 1981) assuming an attractive electron–target potential, so that an electron scattered through a positive angle can readily transfer positive angular momentum to the target as it loses energy. This argument clearly fails for larger angles, beyond about 30° to 50°. The structural features of the two curves, for example the zero crossing, generally occur at smaller angles for the higher energy. This was also noted in the comparison of earlier NIST data at 20 and 54.4 eV (McClelland *et al* 1989).

The theoretical calculations of Mitroy *et al* (1987), based on a four-state close-coupling (4CC) model, are also shown in figure 2(*a*) for 10 eV. The agreement is qualitatively very good although some discrepancies exist. Theoretical data were unavailable for comparison at 40 eV.

Considering $L_\perp^{\mathrm{T}}$ and $L_\perp^{\mathrm{S}}$ for the separate spin channels, in figures 2(*b*) and 3(*b*), significant differences between triplet and singlet can be seen for 10 eV while spin has only a small role in the angular momentum transfer process at 40 eV. The 4CC calculations show even better agreement with the triplet channel than with the spin-averaged $L_\perp$, while the singlet agreement is poor. It seems that the discrepancies between theory and experiment for the unpolarized $L_\perp$ can be largely accounted for by the disagreement in the singlet channel. In an unpolarized experiment, the incident and bound electrons are three times more likely to couple in a triplet state than a singlet, and hence the spin-averaged $L_\perp$ is dominated by the triplet $L_\perp^{\mathrm{T}}$ which is well predicted by the theory.

The ratio, *r*, of triplet to singlet differential cross sections is shown in figures 2(*c*) and 3(*c*). These depend on M_L-substate averages, rather than on substate differences as in the $L_\perp$ case. The ratios are generally greater than one, indicating that triplet scattering is dominant. The curve at 10 eV shows the 4CC results, which do not agree well with the experimental data. While the theory indicates dominance of the singlet channel at forward angles, the experiment shows the opposite. At backward angles there is some qualitative agreement between theory and experiment, although the magnitude of *r* differs by as much as a factor of two.

The reduced spin effects seen at higher energy are to be expected because exchange effects become smaller due to shorter collision time and/or less overlap of the incident and bound electronic wavefunctions. These arguments do not, however, provide a good predictor at low energies, as discussed by McClelland *et al* (1989). This point is illustrated by figure 4, which shows the results of McClelland *et al* at 20 eV. The data are shown with the 4CC results of Mitroy *et al* (1987) (communicated privately), and it is apparent that the spin channel ratio *r* is of a similar magnitude to that at 10 eV despite the factor of two in energy. Comparison is also made with the distorted wave calculations of Purohit and Mathur (1990) at 20 eV but agreement is less satisfactory.

These measurements complete a series of detailed studies of spin-resolved electron–sodium scattering. Data have been presented at 10 and 40 eV which complement earlier results at 4.1 and 20 eV, and corresponding elastic scattering data at 4.1, 10 and 20 eV (Lorentz *et al* 1991), thereby spanning most of the energy range where exchange effects are likely to be important. These effects are substantial in all cases and illustrate the need for careful treatment of exchange in any calculation. Close-coupling theory shows considerable promise, although significant discrepancies are observed in comparison

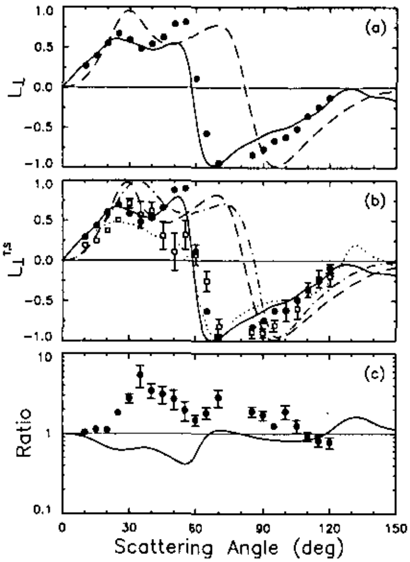

Figure 4. Superelastic electron–sodium scattering with 20 eV total energy. (*a*) Spin-averaged angular momentum transfer, $L_\perp$: ●, present results; ——, 4CC (Mitroy *et al* 1987); – – – –, $L_\perp^T$ (Purohit and Mathur 1990). (*b*) Spin-resolved angular momentum transfer, $L_\perp^T$ and $L_\perp^S$: ●, $L_\perp^T$ present results; □, $L_\perp^S$ present results; ——, $L_\perp^T$ 4CC (Mitroy *et al* 1987); · · · ·, $L_\perp^S$ 4CC (Mitroy *et al* 1987); – – – –, $L_\perp^T$ (Purohit and Mathur 1990); — · —, $L_\perp^S$ (Purohit and Mathur 1990). (*c*) Triplet-to-singlet ratio, *r*: ●, present results; ——, 4CC (Mitroy *et al* 1987).

with the detailed spin-resolved parameters measured here. The failure is particularly noticeable for the triplet to singlet ratio *r*, emphasizing the value of such detailed measurements which depend on specific channel scattering amplitudes rather than on averages.

This work has been supported in part by the US Department of Energy, Office of Energy Research, Division of Chemical Sciences.

References

Andersen N, Gallagher J W and Hertel I V 1988 *Phys. Rep.* **165** 1–188
Balashov V V, Grum-Grzhimailo A N and Klochkova O I 1989 *J. Phys. B: At. Mol. Opt. Phys.* **22** L669–74
Enemark E A and Gallagher A 1972 *Phys. Rev.* A **6** 192–205
Hermann H W and Hertel I V 1982b *Comment. At. Mol. Phys.* **12** 61–84
Hertel I V, Kelley M H and McClelland J J 1987 *Z. Phys.* D **6** 163–83
Hertel I V and Stoll W 1974 *J. Phys. B: At. Mol. Opt. Phys.* **7** 583–92
Hodge L A, Moravec T J, Dunning F B and Walters G K 1979 *Rev. Sci. Instrum.* **50** 5–8
Kennedy J V, Myerscough V P and McDowell M R C 1977 *J. Phys. B: At. Mol. Phys.* **10** 3759–80
Kessler J 1985 *Polarized Electrons* 2nd edn (Berlin: Springer)
Kohmoto M and Fano U 1981 *J. Phys. B: At. Mol. Phys.* **14** L447–51
Lorentz S R and Miller T M 1991 *Phys. Rev.* A in press
Lorentz S R, Scholten R E, McClelland J J, Kelley M H and Celotta R J 1991 *Phys. Rev.* A in press
McClelland J J, Kelley M H and Celotta R J 1989 *Phys. Rev.* A **40** 2321–9
Mitroy J, McCarthy I E and Stelbovics A 1987 *J. Phys. B: At. Mol. Phys.* **20** 4827–50
Moores D L and Norcross D W 1972 *J. Phys. B: At. Mol. Phys.* **5** 1482–505

Percival I C and Seaton M J 1958 *Phil. Trans. R. Soc.* A **251** 113–38
Purohit S P and Mathur K C 1990 *J. Phys. B: At. Mol. Opt. Phys.* **23** L473–81
Shuttleworth T, Newell W R and Smith A C H 1977 *J. Phys. B: At. Mol. Phys.* **10** 1641–51
Slevin J A and Chwirot S 1990 *J. Phys. B: At. Mol. Opt. Phys.* **23** 165–210
Srivastava S K and Vušković L 1980 *J. Phys. B: At. Mol. Phys.* **13** 2633–43
Teubner P J O, Riley J L, Brunger M J and Buckman S J 1986 *J. Phys. B: At. Mol. Phys.* **19** 3313–26